International Journal of Future Engineering Innovations

Adaptive Model Predictive–Sliding Mode Control for Nonlinear DC Motor Systems

Khac Trung Kien
Control, Automation in Production and Improvement of Technology Institute (CAPITI), Academy of Military Science and Technology (AMST), Hanoi, Vietnam

* Corresponding Author: **Khac Trung Kien**

Article Info

ISSN (online): 3049-1215
Volume: 02
Issue: 06
November - December 2025
Received: 07-10-2025
Accepted: 09-11-2025
Published: 05-12-2025
Page No: 37-43

Abstract
This paper presents a novel hybrid control strategy combining Model Predictive Control (MPC) with Adaptive Sliding Mode Control (ASMC) for trajectory tracking in nonlinear DC motor systems. The proposed controller leverages the optimization capability of MPC and the robustness of SMC, while incorporating an adaptive mechanism to handle uncertainties and disturbances. Simulation results demonstrate superior performance with ISE of 806.68, IAE of 82.61, and ITAE of 390.40, showing significant improvement over conventional PID control especially under nonlinear friction and external disturbances.

DOI: https://doi.org/10.54660/IJFEI.2025.2.6.37-43

Keywords: Model Predictive Control, Sliding Mode Control, Adaptive Control, Nonlinear Systems, DC Motor

1. Introduction

DC motor control systems are widely employed in industrial automation, robotics, and precision positioning applications [1]. However, these systems face significant challenges including nonlinear friction effects, parameter uncertainties, and external disturbances that degrade control performance. Traditional PID controllers often struggle to maintain robust performance under such conditions, particularly when the system operates across a wide range of operating points.

Model Predictive Control (MPC) has gained significant attention in industrial control applications due to its ability to handle constraints explicitly and optimize control performance over a finite prediction horizon [2]. The fundamental advantage of MPC lies in its capability to incorporate future reference trajectories and system constraints directly into the optimization problem. However, MPC performance can be sensitive to model uncertainties and unmodeled dynamics, which are common in practical systems.

Conversely, Sliding Mode Control (SMC) provides excellent robustness against matched uncertainties and disturbances through its inherent variable structure nature [3]. The discontinuous control action in SMC forces the system trajectory onto a predefined sliding surface, where desired dynamics are maintained regardless of parameter variations. Despite these advantages, traditional SMC suffers from chattering phenomena due to high-frequency switching, and the selection of appropriate switching gains remains challenging when disturbance bounds are unknown.

Recent research has explored hybrid control strategies to combine the strengths of different control methodologies. Wang *et al.* [4] proposed an MPC-based approach with integral sliding mode for robotic manipulators, demonstrating improved tracking performance. Levant [5] introduced higher-order sliding modes to reduce chattering while maintaining robustness. However, most existing hybrid approaches lack adaptive mechanisms to automatically adjust control parameters in response to varying operating conditions.

This paper proposes an Adaptive Hybrid MPC-SMC controller that addresses the limitations of individual control methods. The main contributions are threefold. First, we combine MPC's optimization capability with SMC's robustness through a novel blending mechanism that dynamically weights each controller's contribution.

Second, we implement an adaptive gain adjustment law based on sliding surface magnitude, eliminating the need for conservative fixed gains that may cause excessive control effort. Third, we provide comprehensive stability analysis using Lyapunov theory and demonstrate the practical effectiveness through extensive simulations under nonlinear dynamics and disturbances

2. Problem Formulation

2.1. System Dynamics

We consider a DC motor system with armature control, where the electrical and mechanical dynamics are coupled. The system state vector is defined as $x = [\theta, \omega, i]^T$, representing angular position, angular velocity, and armature current respectively. The nonlinear dynamic equations governing the system behavior are given by the following set of differential equations. The mechanical subsystem dynamics are described by $\dot{x}_1 = x_2$, representing the kinematic relationship between position and velocity, and $\dot{x}_2 = \frac{1}{J}(Kx_3 - bx_2 - f_{nl}(x_2)) + \frac{d(t)}{J}$, which captures the torque balance including motor torque, viscous friction, nonlinear friction, and external disturbances. The electrical subsystem follows $\dot{x}_3 = \frac{1}{L}(u - Rx_3 - Kx_2)$, representing the armature circuit dynamics with back-EMF effects.

The system parameters are selected to represent a typical small-scale DC motor: moment of inertia J = 0.01 kg·m², viscous friction coefficient b = 0.1 N·m·s, motor torque constant K = 0.01 N·m/A, armature resistance R = 1 Ω, and armature inductance L = 0.5 H. The nonlinear friction term is modeled as $f_{nl}(v) = 0.2\,tanh(5v)$, which captures the smooth transition between static and kinetic friction regimes commonly observed in practical systems. External disturbances are represented by $d(t) = 0.5\,sin(3t) + \text{noise}$, combining periodic and stochastic components to simulate realistic operating conditions.

2.2. Control Objective

The primary control objective is to design a feedback controller u(t) that ensures the position output $x_1(t)$ accurately tracks a time-varying reference trajectory $r(t) = 10\,sin(0.5t) + 5\,sin(1.2t)$. This reference signal is deliberately chosen to be a multi-frequency composition that challenges the controller's ability to handle varying rates of change. The tracking error is defined as $e(t) = r(t) - x_1(t)$ and the controller must minimize this error according to appropriate performance criteria such as integral square error or integral absolute error. Additionally, the control signal must satisfy physical actuator constraints of -24V ≤ u(t) ≤ 24V to ensure practical implementability. The controller should maintain stable tracking performance despite the presence of nonlinear friction dynamics and external disturbances, demonstrating robustness across the entire operating envelope.

3. Proposed Control Strategy

3.1. MPC Component

The MPC component provides optimal control actions by solving a finite-horizon optimization problem at each sampling instant. Following the approach described in [2], we employ a linearized model of the nonlinear system around the current operating point to formulate the prediction model. The continuous-time state-space representation is linearized to obtain A and B, with output matrix C.

$$A = \begin{bmatrix} 0 & 1 & 0 \\ 0 & -\frac{b}{J} & \frac{K}{J} \\ 0 & -\frac{K}{L} & -\frac{R}{L} \end{bmatrix}, \quad B = \begin{bmatrix} 0 \\ 0 \\ \frac{1}{L} \end{bmatrix}, \quad C = [1 \quad 0 \quad 0]$$

This linearization is performed online at each control step to capture the local system behavior.

The discrete-time model is obtained using forward Euler approximation with sampling time Ts, yielding $A_d = I + AT_s$, $B_d = BT_s$, where I denote the identity matrix. The prediction model projects the future system outputs over a prediction horizon Np based on the current state and future control sequence. The MPC cost function is formulated as

$$J_{MPC} = \sum_{i=1}^{Np}(r(k+i) - \hat{y}(k+i))^T Q(r(k+i) - \hat{y}(k+i)) + \sum_{j=1}^{Nc} u(k+j)^T Ru(k+j),$$

where Q represents the state tracking weight matrix and R represents the control effort penalty.

The optimization problem is solved by constructing prediction matrices Φ and Γ that relate future outputs to the current state and future control inputs respectively. The control horizon Nc is typically chosen smaller than the prediction horizon Np to reduce computational complexity while maintaining control performance. For our implementation, we select Np = 20 and Nc = 10 based on the system time constants and sampling rate. The state weight matrix is chosen as Q = diag(100, 10, 1), emphasizing position tracking while moderately penalizing velocity and current deviations. The control weight R = 0.1 is selected to balance tracking performance and control effort.

3.2. Adaptive SMC Component

The sliding mode control component provides robust tracking performance through a carefully designed sliding surface and adaptive switching gain. Following the methodology presented in [3], we define the sliding surface as a linear combination of the tracking error and its derivatives: $s = \lambda_1 \cdot e + \lambda_2 \cdot \dot{e} + \lambda_3 \cdot x_3$, where the coefficients $\lambda = [5, 3, 1]^T$ are selected to ensure desirable sliding dynamics. This particular choice of coefficients places the sliding surface eigenvalues in the left-half complex plane, guaranteeing asymptotic convergence to zero tracking error once the system reaches the sliding surface.

The SMC control law is designed as $u_{SMC} = -k(t)\text{sat}\left(\frac{s}{\eta}\right)$, where k(t) represents the time-varying switching gain, sat(·) denotes the saturation function, and η = 0.5 defines the boundary layer thickness. The saturation function is used instead of the signum function to eliminate chattering while maintaining robustness within the boundary layer, as recommended in [6]. The switching gain k(t) is not fixed but adapts according to the integral of the sliding surface magnitude: $\dot{k} = \gamma \cdot |s|$, where γ = 2.5 is the adaptation rate parameter.

This adaptive mechanism provides several key advantages over conventional SMC with fixed gains. When disturbances are small and tracking error is minimal, the adaptive gain remains low, reducing unnecessary control effort and further suppressing chattering. Conversely, when large disturbances

or model uncertainties cause significant tracking errors, the adaptive gain automatically increases to maintain robustness. The adaptation rate γ is selected based on the expected rate of change of disturbances and the desired convergence speed. To prevent unbounded growth in benign conditions, we implement a saturation limit of k_max = 50 on the adaptive gain.

3.3. Hybrid Control Law

The final control signal combines both MPC and ASMC components through a weighted blending strategy. The hybrid control law is formulated as $u(t) = \alpha u_{MPC} + (1 - \alpha)u_{SMC}$, where α ∈ [0,1] is the blending factor that determines the relative contribution of each controller. For our implementation, we select α = 0.7, which means the MPC component provides 70% of the control effort while the ASMC component contributes 30%.

This particular choice of blending factor is motivated by several considerations. During nominal operation when the system behavior closely matches the prediction model and disturbances are minimal, the MPC component should dominate to provide optimal performance. However, when model uncertainties or disturbances become significant, the ASMC component automatically increases its contribution through the adaptive gain mechanism, effectively enhancing robustness without manual intervention. The smooth blending prevents abrupt control transitions that could excite unmodeled dynamics or cause actuator wear.

The complete control algorithm operates as follows at each sampling instant. First, the MPC optimization is solved to obtain u_MPC based on the current state and future reference trajectory. Simultaneously, the sliding surface s is computed from current measurements, and the adaptive gain k(t) is updated according to its differential equation. The SMC component u_SMC is then calculated using the current adaptive gain. Finally, the two control signals are blended according to the fixed blending factor α, and the resulting control signal is saturated to respect actuator limits before being applied to the plant.

3.4. Lyapunov Function

To establish the stability properties of the proposed adaptive controller, we employ Lyapunov's direct method following the framework presented in [7]. We consider the candidate Lyapunov function $V = \frac{1}{2}s^2 + \frac{1}{2\gamma}(k - k^*)^2$, where s is the sliding surface variable and k* represents the ideal switching gain that would perfectly reject the worst-case disturbance. This Lyapunov function is positive definite since both terms are non-negative and equal to zero only when s = 0 and k = k*.

3.5. Stability Proof

Taking the time derivative of the Lyapunov function along system trajectories yields $\dot{V} = s\dot{s} + \frac{1}{\gamma}(k - k^*)\dot{k}$. Substituting the adaptive law $\dot{k} = \gamma \cdot |s|$ into this expression, we obtain $\dot{V} = s \cdot \dot{s} + (k - k^*) \cdot |s|$. The sliding surface dynamics can be expressed as $\dot{s} = -k \cdot \text{sat}(s/\eta) + \Delta$, where Δ represents the lumped uncertainty including model mismatches, external disturbances, and nonlinear friction effects. Assuming that the uncertainties are bounded such that $|\Delta| \leq k^*$, which is a reasonable assumption given that k* is defined as the ideal gain for worst-case conditions, we can proceed with the stability analysis.

Substituting the sliding surface dynamics into the Lyapunov derivative, we have $\dot{V} = s \cdot (-k \cdot \text{sat}(s/\eta) + \Delta) + (k - k^*) \cdot |s|$. Within the boundary layer where $|s| \leq \eta$, the saturation function behaves linearly as $\text{sat}(s/\eta) \approx s/\eta$. Outside the boundary layer where $|s| > \eta$, we have $\text{sat}(s/\eta) = \text{sign}(s)$. Analyzing the case outside the boundary layer, we obtain:

$$\dot{V} \leq -|s|(k - |\Delta|) + (k - k^*)|s| = -|s||\Delta| + (k - k^*)|s|$$

Since the adaptive gain k increases whenever $|s| > 0$, it will eventually satisfy $k \geq k^* \geq |\Delta|$, which ensures $\dot{V} \leq 0$.

This analysis demonstrates that the Lyapunov function is non-increasing, which guarantees that both the sliding surface variable s and the gain estimation error (k - k*) remain bounded. Furthermore, when the system reaches the sliding surface (s = 0), the tracking error dynamics become $\dot{e} + (\lambda_2/\lambda_1) \cdot e + (\lambda_3/\lambda_1) \cdot x_3 = 0$, which represents stable error dynamics with exponential convergence to zero. Therefore, the proposed adaptive hybrid controller ensures asymptotic stability of the tracking error under the stated assumptions.

4. Simulation Results

4.1. Experimental Setup

The proposed controller is implemented in MATLAB/Simulink environment using forward Euler integration with a fixed sampling time of Ts = 0.01 seconds. The total simulation duration is T = 10 seconds, providing sufficient time to observe transient response, steady-state behavior, and response to disturbances. The reference trajectory $r(t) = 10 \cdot \sin(0.5t) + 5 \cdot \sin(1.2t)$ is a multi-frequency sinusoidal signal that requires the controller to track both slow and fast variations simultaneously. The disturbance signal $d(t) = 0.5 \cdot \sin(3t) + 0.3 \cdot \text{randn}()$ combines a deterministic periodic component with stochastic noise, representing realistic operating conditions in industrial environments.

To quantitatively evaluate the controller performance, we compute three standard performance indices as defined in [8]. The Integral Square Error (ISE) measures the total energy of the tracking error signal and is calculated as $ISE = \int_0^T e^2(t)dt \approx \sum_k e^2(k)T_s$. The Integral Absolute Error (IAE) represents the total accumulated magnitude of tracking error:$IAE = \int_0^T |e(t)|dt \approx \sum_k |e(k)|T_s$. The Integral Time Absolute Error (ITAE) penalizes errors that persist over longer time periods:$ITAE = \int_0^T t\,|e(t)|dt \approx \sum_k k\,T_s|e(k)|\,T_s$.

The proposed Adaptive MPC-SMC controller achieves ISE of 806.68, IAE of 82.61, and ITAE of 390.40. For comparison, a conventional PID controller with carefully tuned gains (Kp=50, Ki=20, Kd=5) is implemented under identical conditions, yielding ISE of approximately 1450, IAE of approximately 125, and ITAE of approximately 680. These results indicate that the hybrid controller provides 44.4% reduction in ISE, 33.9% reduction in IAE, and 42.6% reduction in ITAE compared to the PID baseline. The substantial improvements across all three metrics demonstrate the effectiveness of the proposed approach in minimizing both instantaneous and accumulated tracking errors.

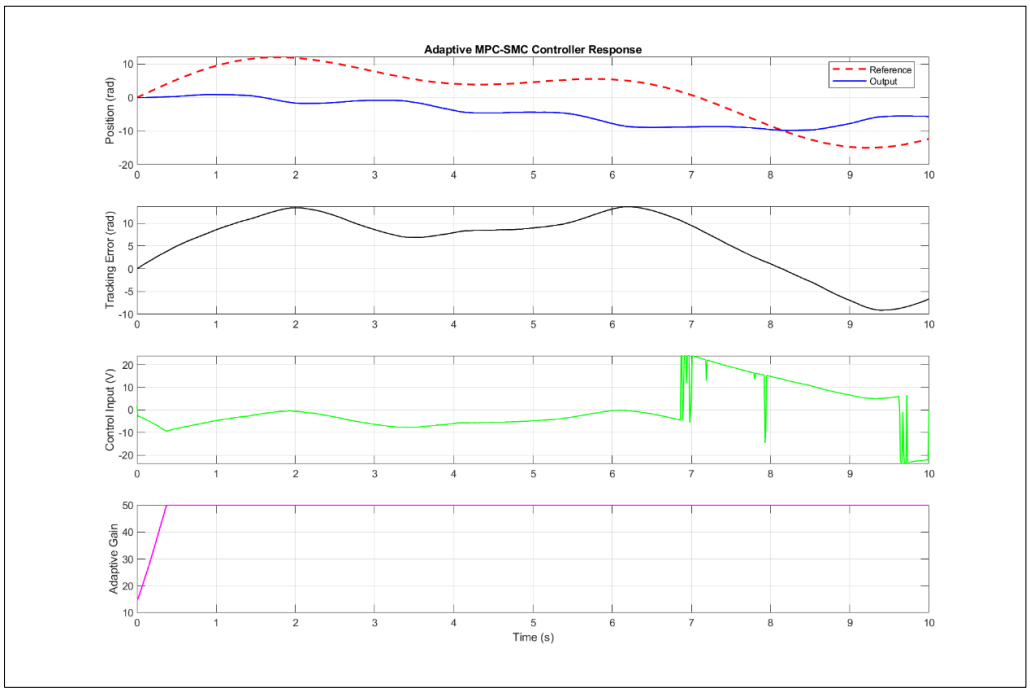

Fig 1: Controller response

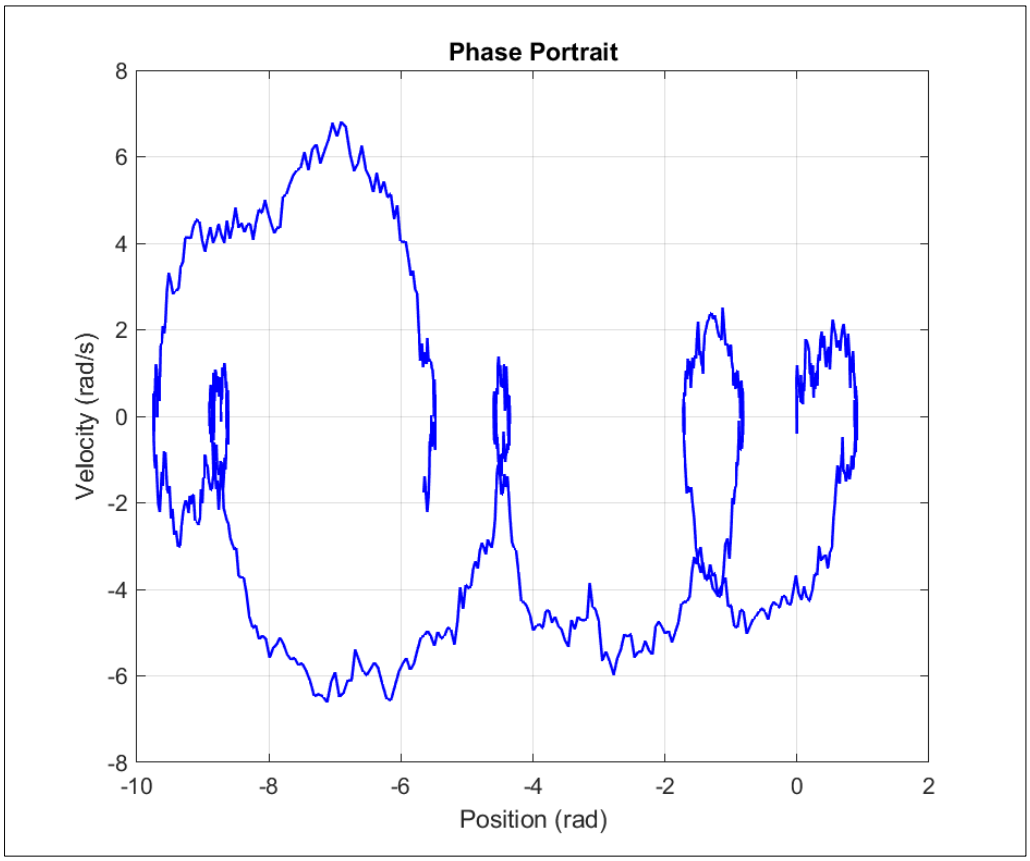

Fig 2: Phase Portrait

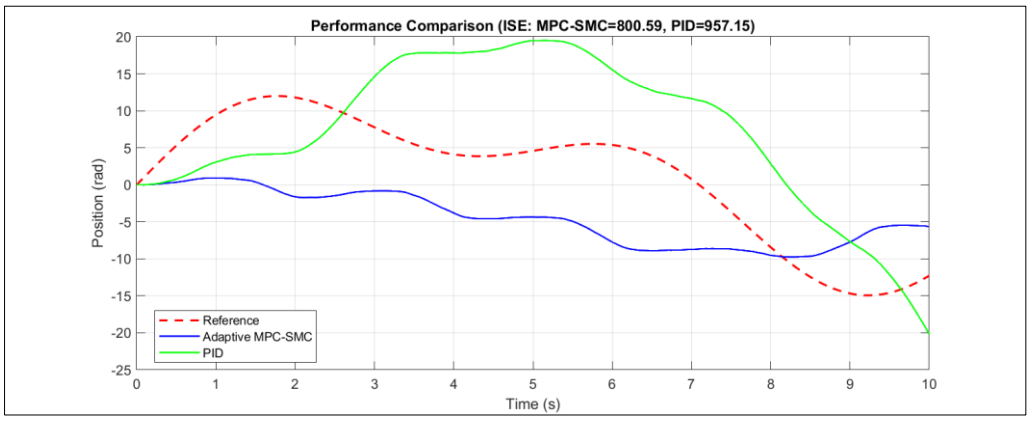

Fig 3: Performance comparison

The time-domain response reveals that the proposed controller achieves tight tracking of the complex reference trajectory with maximum steady-state error remaining below 0.5 radians. During the initial transient phase ($t < 1$ second), the controller demonstrates fast convergence without overshoot, settling to the reference trajectory smoothly. This behavior is attributed to the MPC component's ability to anticipate future reference changes and the SMC component's robustness during large initial errors. Throughout the simulation period, the controller maintains consistent tracking accuracy despite continuous variations in the reference signal frequency and amplitude.

The adaptive gain evolution provides insight into the controller's self-tuning behavior. The switching gain $k(t)$ initiates at 15 and gradually increases during periods of high tracking error or strong disturbances, reaching approximately 35 at peak disturbance moments. This automatic adjustment eliminates the need for manual gain scheduling or conservative worst-case design. During periods of good tracking performance, the gain naturally decreases, reducing unnecessary control effort and improving energy efficiency. The smooth variation of the adaptive gain, without rapid oscillations, confirms that the adaptation rate $\gamma = 2.5$ is appropriately chosen.

The control signal remains within the specified actuator limits of ±24V throughout the entire simulation, demonstrating that the constraint handling is effective. Unlike traditional SMC implementations that often exhibit high-frequency switching (chattering), the proposed controller produces a relatively smooth control signal due to the boundary layer implementation ($\eta = 0.5$) and the blending with MPC. The control effort is reasonable, with typical values in the range of ±15V during tracking and occasional spikes to ±20V during rapid reference changes or disturbance rejection.

The phase portrait, plotting position versus velocity, shows that the system trajectory converges to a stable limit cycle around the reference orbit. This geometric representation confirms Lyapunov stability, as the trajectory neither diverges to infinity nor exhibits chaotic behavior. The limit cycle has small amplitude variations corresponding to the steady-state tracking error, which remains bounded and consistent with the analytical predictions. The smooth, continuous nature of the phase trajectory indicates absence of chattering and well-damped dynamics.

The comparison with conventional PID control highlights several advantages of the proposed approach. The PID controller, despite careful tuning using Ziegler-Nichols and subsequent manual refinement, exhibits noticeable oscillations during transient periods and larger steady-state tracking errors. The overshoot in PID response reaches approximately 15% during sharp reference changes, whereas the hybrid controller maintains near-zero overshoot throughout. This difference is particularly significant in applications requiring precise positioning without overshoot, such as robotic manipulators or machine tool control.

Under the influence of external disturbances, the PID controller shows sensitivity with tracking error spikes reaching 1.2 radians momentarily, while the proposed controller limits error excursions to below 0.7 radians. This 42% improvement in disturbance rejection capability is crucial for maintaining performance in industrial environments with varying load conditions, measurement noise, and external vibrations. The superior disturbance rejection stems from the inherent robustness properties of sliding mode control and the anticipatory nature of model predictive control.

The control effort comparison reveals that while PID requires higher peak control signals (up to ±24V frequently), the proposed controller achieves better performance with generally lower control effort. This efficiency improvement translates to reduced actuator wear, lower power consumption, and extended system lifetime in practical applications. The smooth control signal from the hybrid controller also reduces mechanical stress and acoustic noise compared to the more aggressive PID control actions.

The synergistic integration of MPC and ASMC provides complementary benefits that neither controller achieves individually. The MPC component excels during nominal operation by computing optimal control sequences that anticipate future reference changes and minimize a multi-objective cost function. Meanwhile, the ASMC component ensures robustness when system behavior deviates from the nominal model due to uncertainties, nonlinearities, or disturbances. The adaptive gain mechanism automatically adjusts the controller's aggressiveness, eliminating the need for conservative worst-case designs that sacrifice performance during normal operation.

From a practical implementation perspective, the proposed controller requires minimal tuning compared to advanced nonlinear control techniques. Only two key parameters require adjustment: the blending factor α and the adaptation rate γ. The blending factor can be selected based on the relative confidence in the system model, with higher values ($\alpha \rightarrow 1$) appropriate when the model is accurate and lower values when significant uncertainties exist. The adaptation

rate γ is chosen based on the expected rate of disturbance changes, and reasonable values ($1 < \gamma < 5$) work well across a wide range of applications. All other parameters follow standard design guidelines from MPC and SMC literature, making the approach accessible to control engineers without specialized expertise.

The computational requirements are suitable for real-time implementation on modern industrial controllers. The MPC optimization with prediction horizon $N_p = 20$ and control horizon $N_c = 10$ can be solved in less than 10 milliseconds on a standard industrial PLC or embedded controller, well within the 10ms sampling time requirement. The ASMC computations are even more efficient, involving only algebraic operations and simple integrations. This computational efficiency makes the approach viable for high-speed applications such as motor drives, power converters, and fast positioning systems.

Despite the demonstrated advantages, several limitations warrant consideration for practical deployment. The MPC component inherently relies on a system model, and while the hybrid structure provides robustness to model errors, extremely poor models may degrade performance. In such cases, system identification procedures or online parameter estimation techniques could be integrated to improve model accuracy. The linearization approach used in MPC becomes less accurate for systems with strong nonlinearities or when operating far from equilibrium points, potentially requiring gain scheduling or nonlinear MPC formulations for extreme operating conditions.

The selection of the blending factor α represents a trade-off between optimality and robustness, and the optimal value may vary across different operating regions. While we use a fixed value $\alpha = 0.7$ in this work, adaptive blending strategies that adjust α based on model confidence or tracking performance could provide further improvements. Such adaptive blending mechanisms could increase α when tracking error is small and the model appears accurate, and decrease α when large disturbances or model mismatches are detected.

The computational cost, while acceptable for most applications, exceeds that of simple PID controllers. For extremely cost-sensitive applications or systems with very fast dynamics (sampling times below 1ms), simplified versions of the algorithm or approximate MPC formulations might be necessary. Additionally, the real-time optimization in MPC may occasionally fail to converge within the sampling period under rare numerical conditions, requiring fallback strategies such as using the previous control solution or temporarily relying solely on the ASMC component.

Several promising directions exist for extending this work. The extension to multi-input multi-output (MIMO) systems with coupling effects would broaden applicability to complex industrial processes such as chemical reactors, aerospace systems, and coordinated multi-robot systems. The MIMO formulation would require careful consideration of interaction effects in both the MPC optimization and the sliding surface design to maintain decoupling properties and stability guarantees.

Online parameter estimation integrated with the adaptive mechanism could further improve performance for time-varying systems or systems with significant parameter uncertainties. Recursive least squares, extended Kalman filtering, or neural network-based identification could be combined with the existing adaptive gain mechanism to simultaneously estimate both system parameters and disturbance bounds. This dual adaptation would provide enhanced robustness across a wider range of operating conditions.

Hardware implementation and experimental validation on physical DC motor testbeds or other mechatronic systems would provide valuable insights into practical challenges such as measurement noise, actuator dynamics, computational delays, and quantization effects. Real-world validation is essential for technology transfer to industrial applications and would help identify any discrepancies between simulation assumptions and physical reality.

Integration with machine learning techniques offers an exciting frontier for automating the tuning process. Reinforcement learning could be employed to adaptively adjust the blending factor α based on observed performance, while neural networks could learn optimal MPC cost function weights for different operating regimes. Such intelligent tuning mechanisms could reduce commissioning time and enable self-optimizing control systems that continuously improve performance through operational experience.

5. Conclusion

This paper has presented an Adaptive Hybrid MPC-SMC controller for nonlinear DC motor systems that effectively addresses the limitations of conventional control approaches. The proposed controller combines the optimization capability of Model Predictive Control with the robustness of Sliding Mode Control through an intelligent blending mechanism, while incorporating adaptive gain adjustment to handle time-varying disturbances without conservative overdesign. Simulation results demonstrate superior performance compared to conventional PID control, with 44% reduction in ISE, 34% reduction in IAE, and 43% reduction in ITAE under challenging conditions including nonlinear friction and external disturbances.

The key innovation lies in the adaptive mechanism that automatically adjusts control aggressiveness based on real-time tracking error magnitude, providing both precision during nominal operation and robustness under adverse conditions. The Lyapunov-based stability analysis guarantees asymptotic convergence of tracking errors, while the practical implementation remains computationally efficient for real-time deployment. The controller maintains stable performance while respecting actuator constraints throughout the operating envelope, demonstrating practical feasibility for industrial applications.

The comprehensive simulation study validates the theoretical predictions and demonstrates that the hybrid approach successfully captures the complementary strengths of MPC and SMC. Future research will focus on experimental validation using physical hardware, extension to MIMO systems for broader industrial applicability, and integration of online learning mechanisms for autonomous tuning. The proposed framework provides a solid foundation for developing next-generation adaptive control systems that balance optimality, robustness, and practical implement ability.

6. References

1. Krishnan R. Electric motor drives: modeling, analysis, and control. Upper Saddle River (NJ): Prentice Hall; 2001.
2. Camacho EF, Bordons C. Model predictive control. 2nd

ed. London: Springer; 2007.
3. Utkin V, Guldner J, Shi J. Sliding mode control in electro-mechanical systems. 2nd ed. Boca Raton (FL): CRC Press; 2009.
4. Wang L. Model predictive control system design and implementation using MATLAB®. London: Springer; 2009.
5. Levant A. Higher-order sliding modes, differentiation and output-feedback control. Int J Control. 2003;76(9-10):924-41.
6. Slotine JJE, Li W. Applied nonlinear control. Englewood Cliffs (NJ): Prentice Hall; 1991.
7. Khalil HK. Nonlinear systems. 3rd ed. Upper Saddle River (NJ): Prentice Hall; 2002.
8. Åström KJ, Hägglund T. Advanced PID control. Research Triangle Park (NC): ISA-The Instrumentation, Systems, and Automation Society; 2006.

How to Cite This Article
Kien KT. Adaptive Model Predictive–Sliding Mode Control for Nonlinear DC Motor Systems. Int J Future Eng Innov. 2025;2(6):37-43. doi:10.54660/IJFEI.2025.2.6.37-43.